

Probing the non-Debye low frequency excitations in glasses through random pinning

Luca Angelani^{a,b}, Matteo Paoluzzi^c, Giorgio Parisi^{b,d,e}, and Giancarlo Ruocco^{b,f}

^aISC-CNR, Institute for Complex Systems, Piazzale A. Moro 2, I-00185 Roma, Italy; ^bDipartimento di Fisica, Sapienza Università di Roma, Piazzale A. Moro 2, I-00185, Rome, Italy; ^cDepartment of Physics and Syracuse Soft & Living Matter Program, Syracuse University, Syracuse NY 13244, USA; ^dNanotec-CNR, UOS Rome, Sapienza Università di Roma, Piazzale A. Moro 2, I-00185, Rome, Italy; ^eINFN-Sezione di Roma 1, Piazzale A. Moro 2, 00185, Rome, Italy; ^fCenter for Life Nano Science, Istituto Italiano di Tecnologia, Viale Regina Elena 291, I-00161, Rome, Italy

March 16, 2018

We investigate the properties of the low-frequency spectrum in the density of states $D(\omega)$ of a three dimensional model glass former. To magnify the Non-Debye sector of the spectrum, we introduce a random pinning field that freezes a finite particle fraction in order to break the translational invariance and shifts all the vibrational frequencies of the extended modes towards higher frequencies. We show that Non-Debye soft localized modes progressively emerge as the fraction p of pinned particles increases. Moreover, the low-frequency tail of $D(\omega)$ goes to zero as a power law $\omega^{\delta(p)}$, with $2 \leq \delta(p) \leq 4$ and $\delta = 4$ above a threshold fraction p_{th} .

glasses | normal modes | non-Debye law | soft modes

Understanding the peculiarities and the universal features of the low-frequency spectrum in glasses plays a crucial role to gain insight into their thermal and mechanical properties.

In the case of crystalline solids, mechanical and thermal properties follow universal laws that can be obtained through Debye's theory. Debye's law assumes that the only energy excitations around the ground state in crystals are phonons, i. e., Goldstone modes. The corresponding density of states $D(\omega)$ below Debye's frequency follows $D(\omega) \sim \omega^{d-1}$, in d spatial dimensions (1).

More complex is the situation for amorphous systems where the low-frequency spectrum shows an abundance of soft non-Goldstone modes. Quasilocalized soft modes are involved, for example, in the relaxation processes of supercooled liquid (2), and in the plastic flow of disordered solids (3). They have a natural interpretation within the jamming transition. At the jamming point, a glass is isostatic, i. e., the number of degrees of freedom equals the number of constraints (4, 5). This means that soft modes are induced as soon as a particle contact is removed. More in general, thanks to a class of exactly solvable mean-field models for which it has been proven that the energy landscape is organized into a complex hierarchy of marginally stable states (6–8), marginal stability has been suggested as a general ingredient for the rising of no-energy cost excitations connecting degenerate minima that are separated by small energy barriers (9, 10).

Theoretical models of random media predict a universal law for the density of the states of the non-Goldstone (i.e. non-phononic) component of the spectrum with a scaling $D(\omega) \sim \omega^4$ in any dimensions (11, 12). Consistently, it has been recently shown that in many real and simulated glasses the non-Debye contribution to the density of states is proportional to the phonon damping, thus showing the well known Reyleigh fourth power frequency dependence (13). However, since on large enough scale glasses are continuum media, the

phononic contribution in $D(\omega)$ dramatically overcomes any subdominant non-Goldstone tail at low frequencies (14). Numerical simulations of repulsive binary mixture suggests that the Goldstone modes hybridizes with non-Goldstone excitations and destroys the ω^4 tail (15).

Recently, it has been possible to observe a non-Goldstone low-frequency sector of the spectrum in the density of states of structural glasses and disordered systems that follows a power law $D(\omega) \sim \omega^4$ (16–20). In order to take access to non-Debye modes in numerical models, one has to perform simulations of extremely large system sizes (20). Alternatively, one has to find a protocol to cancel the Goldstone bosons from the low-frequency region (17) by choosing suitably small systems.

In the present paper, in analogy with the procedure adopted in Ref. (16) where a random field has been introduced in the Heisenberg spin-glass to destroy the spin-wave contribution at low frequencies, we employ a random pinning field that freezes a finite fraction of particles. The presence of this random external field destroys any spatial symmetry, removing the corresponding Goldstone excitations.

Random pinning has been largely employed to gain more information about Random-First-Order Theory in glass-forming liquids (21–29). In the following, we will show that random pinning allows also to improve our knowledge about the density of states in amorphous solids.

Here, we perform molecular dynamics simulations of a particulate glass model in three dimensions. After equilibrating the fluid at high temperatures, we compute the density of the states obtained through the normal modes around the

Significance Statement

Amorphous solids are continuum media. However, their mechanical and thermodynamical properties, even though universal, dramatically deviate from those in crystalline solids. Their anomalous behavior reflects peculiar and universal deviations from Debye's law in the low-frequency sector of the density of states $D(\omega)$. Theoretical models predict a population of non-Goldstone bosons following the universal power law $D(\omega) \sim \omega^4$ that are subdominant and then hard to detect. In this work, we introduce a general protocol that can be employed in both, numerical simulations and experiments, to probe the non-Debye portion of the spectrum.

Author contributions: G.P. conceived research; L.A., M.P., G.P., and G.R. designed research; M.P. and G.R. performed research; M.P. wrote the paper.

Please declare any conflict of interest here.

¹ A.O. (Author One) and A.T. (Author Two) contributed equally to this work (remove if not applicable).

² To whom correspondence should be addressed. E-mail: author.twoemail.com

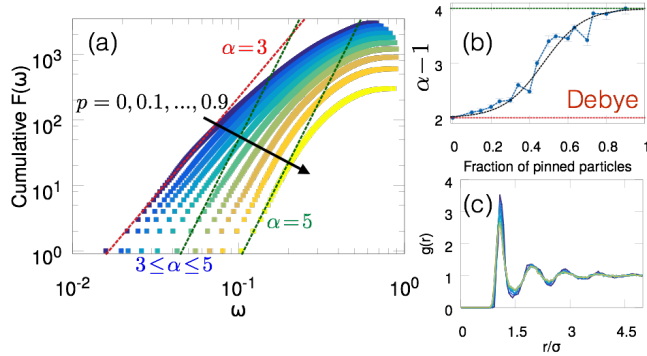


Fig. 1. (a) The cumulative function of the density of states $F(\omega)$ deviates progressively from Debye by increasing the fraction of pinned particles p , from 0 (blue) to 0.9 (yellow). The considered system size is $N = 1000$. (b) From the tail of $F(\omega)$ we fit the exponent α that saturates towards 5 by increasing p . The black dashed curve is the best fit to logistic function. (c) Radial distribution function at different pinned particle fraction, from $p = 0$ (blue) to $p = 0.8$ (yellow).

corresponding inherent structures. In computing the inherent structures, we freeze a particle fraction p . By progressively increasing p , we observe that the resulting low-frequency spectrum qualitatively changes. In particular, it develops a non-Debye tail. We find that the low-frequency spectrum is populated by soft modes that reach zero as a power law $D(\omega) \sim \omega^\delta$. The exponent δ departs continuously from the Debye value $\delta = 2$, that is recovered at small fraction of pinned particles. For large p values, the exponent approaches the limit value $\delta = 4$. Moreover, the non-Goldstone modes become progressively quasilocated as the number of frozen particles increases.

Results

As a model glass former, we consider a binary mixture 50 : 50 composed by soft-sphere in three dimensions. The particles interact each other through an r^{-12} potential. The detail about the model and numerical simulations are given in Materials and Methods. The typical protocol adopted for investigating the vibrational modes are the following. We start with thermalizing a configuration at a high temperature far above the dynamical temperature T_{MC} of the model, i. e., the temperature where the system undergoes a dynamical arrest. The data presented here are obtained working at $T = 3T_{MC}$. The inherent structure of the equilibrated configuration is then computed by minimizing the mechanical energy. In computing the inherent structure, we randomly choose a finite fraction p of particles that is maintained frozen during energy minimization. The vibrational modes are obtained through the diagonalization of the corresponding dynamical matrix.

We start our discussion by considering a system composed by $N = 1000$ particles. Fig. (1)-a shown the cumulative distribution of the density of states $F(\omega)$ – see Materials and Methods. This quantity shows a power law tail at low frequency, $F(\omega) \sim \omega^\alpha$, corresponding to a power law tail of the density of states, $D(\omega) \sim \omega^\delta = \omega^{\alpha-1}$. For $p = 0$, the Debye contribution dominates the low-frequency spectrum below the Boson peak. In that region, the cumulative distribution reaches zero as $F(\omega) \sim \omega^3$, i. e., $\alpha = d$. By increasing the fraction of pinned particles p , we observe a progressively disappearing of the Goldstone sector in favor of non-Goldstone

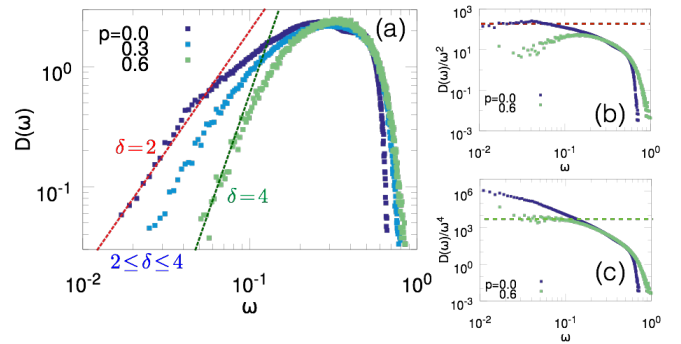


Fig. 2. (a) The density of states $D(\omega)$ for $N = 1000$ particles at $p = 0$ (blue), 0.3 (light-blue), and 0.6 (green). Red dashed curve is Debye's scaling $\sim \omega^2$. The dashed green curve indicates $D(\omega) \sim \omega^4$. Debye and non-Debye spectrum are highlighted in (b) and (c) where we plot $D(\omega)/\omega^2$ and $D(\omega)/\omega^4$, respectively.

modes. The dashed curves are the fit to the power law ω^α , we obtain a monotonic growing of α with increasing p that eventually saturates at the value $\alpha = 5$. The behavior of $\alpha - 1$ as a function of p is shown in Fig. (1)-b. In order to give an estimate for the crossover between Debye and non-Debye regime, we fit the curve $\delta(p) = \alpha(p) - 1$ to a generalized logistic curve $\delta(p) = \delta_{min} + \frac{\delta_{min} - \delta_{max}}{1 + e^{\frac{p - p_{th}}{\sigma}}}$ where $\delta_{min} = 2$, $\delta_{max} = 4$ and p_{th} and σ are the fitting parameters. The parameter p_{th} gives an estimate for the threshold values of p between the two regimes. The logistic curve provides a good fit to the data with $p_{th} = 0.47 \pm 0.01$ (black dashed line in Fig. (1)-b). To be sure that random pinning does not dramatically alterate the structural properties of the glass, we have kept track of the radial distribution function $g(r)$ of the configuration that minimizes the energy. As shown in Fig. (1)-c, where we plot the evolution of $g(r)$ for different values of p , random pinning does not alterate the structure of the system that remains amorphous even at large pinned particle fraction.

In Fig. (2) we show $D(\omega)$ for $N = 1000$ particles and $p = 0, 0.3, 0.6$. Red and green dashed lines in panel (a) are the power laws ω^2 and ω^4 , respectively. Of course, at $p = 0$, the excess of soft-modes before the low-frequency power law is the Boson peak. The two scaling regimes are made more clear in panels (b) and (c), where $D(\omega)/\omega^2$ and $D(\omega)/\omega^4$ for $p = 0, 0.6$ are shown. The dashed lines are a guide to the eye that indicate $D(\omega)/\omega^\delta = const.$

In order to take access to lower frequencies, we perform simulations up to $N = 8000$ particles. The corresponding $F(\omega)$, opportunely normalized with the total number of modes, is shown in Fig. (3). As we can appreciate, normal modes from $N = 512, 1000, 8000$ smoothly connect with each other and the corresponding tail connects continuously with no gap. Again, the exponent of the power law $F(\omega) \sim \omega^\alpha$ depends on p and interpolates between Debye $\alpha = 3$ and non-Debye $\alpha = 5$ as the fraction of frozen particle increases. This finding proves that the low-frequency spectrum probed at the smallest size $N = 512$ is representative also for larger system sizes.

Soft modes in glasses are local excitations responsible for the plastic flow (30–32). Localization can be quantified through the inverse participation ratio $IPR(\omega)$. Delocalized modes cover the entire system and $IPR(\omega) \rightarrow 1/N$. Fully localized modes involve few particles meaning that the corresponding eigenvectors count few components. Localization is then sig-

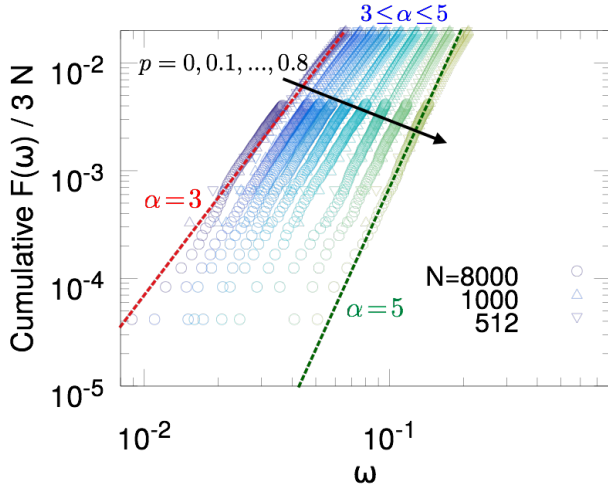


Fig. 3. Normal modes from different system sizes $N = 512, 1000, 8000$ smoothly connect with each other. Red dashed line and green dashed line are a guide to the eye for $F(\omega) \sim \omega^3$ and $F(\omega) \sim \omega^5$, respectively.

naled by a scaling $IPR(\omega) \sim 1$. The $IPR(\omega)$ computed for $N = 1000$ particles is shown in Fig. (4). When $p = 0$, phonons dominate the spectrum, they are extended excitations and, consequently, $IPR \sim 10^{-3} = N^{-1}$. With increasing the fraction of pinned particles, $IPR(\omega)$ increases too. Moreover, localization involves particularly the lowest frequency modes. This is the signal that modes populating the non-Goldstone sector of $D(\omega)$ are progressively quasilocalized in few particle sites.

Summary and Discussion

The anomalous thermal and mechanical properties of glasses are strongly related to their non-Debye excitations that populate the low-frequency spectrum. For this reason, it is crucial to develop techniques and protocols that allow to efficiently probe the sub-dominant glassy modes.

In this paper, we have investigated the low-frequency spectrum of a colloidal glass in three dimensions. In order to gain insight into the non-Debye sector of $D(\omega)$, we employ an external field that randomly freezes a particle fraction. We showed that the random pinning procedure progressively destroys any spatial symmetry presents in the system removing the phononic contribution to $D(\omega)$.

We have also shown that non-Goldstone modes progressively emerge in the spectrum as the fraction of frozen particles increases. Moreover, the power law in the tail of $D(\omega) \sim \omega^\delta$ smoothly changes from Debye, i.e., $\delta = 2$, to $\delta = 4$ at high pinning fraction. The power law $D(\omega) \sim \omega^4$ is fully consistent with the theoretical prediction for Bosonic non-Goldstone excitations given in Ref. (12) that has been also confirmed recently in numerical simulations (16, 17, 20) and in the analysis of the sound attenuation in real and simulated glasses (13). We also found that the low-frequency sector is populated by soft-modes that become progressively localized in few particle sites.

It is worth noting that the scenario here proposed, that is the coexistence at low-frequency of propagating/extended phononic modes with non-Goldstone/localized states, is consistent with the recently developed "Heterogeneous viscoelastic-

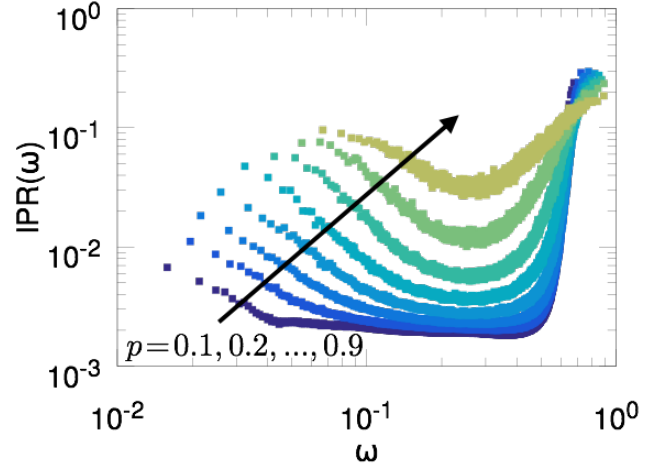


Fig. 4. Inverse participation ratio IPR by increasing the fraction of pinned particles from $p = 0$ (purple) to 0.9 (yellow) for a system size $N = 1000$.

ity" theory (33) where the role of pinning (or of the "external field") is played by the presence of regions with higher elastic moduli in the glass.

As a concluding remark, our study suggests an alternative way to probe the properties of plastic modes in glassy and disordered materials in both, numerical simulations and experiments.

In computer simulations, the protocol considered here has the advantage that works at any system sizes, at least for the repulsive potentials, i. e., colloidal glasses. This suggests that, for instance, it is not necessary to tune the system size below a threshold value as in Ref. (17) or performing large-scale simulations to approach the continuum limit (20).

Moreover, random pinning fields able to trap many colloids through a single laser beam can be generated in a laboratory by means of speckle patterns (34) or by means of suitable algorithms for the control of spatial light modulator to obtain multi-focus beams (35). In that way, it is possible to isolate the non-Goldstone contribution in the low-frequency vibrational modes that are accessible in colloidal glasses by means of confocal microscopy (36).

Materials and Methods

Model. As glass-forming model, we consider a 50:50 binary mixture of large and small soft spheres in three dimensions (37). Indicating with \mathbf{r}_i the position of the particle i , with $i = 1, \dots, N$, two particles i, j interact via a pure repulsive potential $\phi(r_{ij})$, where $r_{ij} \equiv |\mathbf{r}_i - \mathbf{r}_j|$. The potential reads

$$\phi(r_{ij}) = \left(\frac{\sigma_i + \sigma_j}{r_{ij}} \right)^{12} + \alpha r_{ij} + \beta r_{ij}^2, \quad [1]$$

where σ_i takes the value σ_A for the large particles and σ_B for the small ones, with $\sigma_A/\sigma_B = 1.2$ and $\sigma_A + \sigma_B \equiv \sigma = 1$. We consider $N = N_A + N_B$ particles ($N_A = N_B$) that are enclosed in a three dimensional box of side $L = \sigma N^{1/3}$ where periodic boundary conditions are employed. The expression for L guaranties $\rho = N/V = 1$, with ρ the particle density. Moreover, we impose a cutoff to the potential ϕ at $r_c = 1.5/(L/2)$ in a way that $\phi(r) = 0$ for $r > r_c$. The coefficient α and β are chosen in a way such that $\phi(r)$ has continuous first and second derivatives at $r = r_c$.

In the following we report all quantities in reduced units. The MD simulations are performed in *NVT* ensemble at temperature $T = 3T_{MC}$, where T_{MC} is the Mode Coupling temperature of the model, i. e., defined according to $\tau_\alpha(T) \sim (T - T_{MC})^{-\gamma}$, with τ_α the time scale of the α processes. We also performed Swap Monte Carlo Simulations in *NVT* ensemble. In that case, the thermalization of the fluid is controlled looking at the evolution of the total potential energy $\Phi(\{\mathbf{r}_i\}) = \sum_{i \leq j} \phi(r_{ij})$ as a function of temperature and comparing it with the Rosenfeld and Tarazona formula $A + BT^{3/5}$ (38). The system sizes are $N = 512, 1000, 1024, 8000$.

Inherent Structures and Vibrational Mode Analysis. After thermalisation, we compute the corresponding inherent structures that are obtained by minimizing the configurational energy $\Phi(\{\mathbf{r}_i\})$. During the energy minimization, we consider a finite particle fraction pN , with $p \in [0, 1[$, frozen in its equilibrium configuration.

In order to compute the density of states, we expand Φ around the configuration $\{\mathbf{r}_i^0\}$ that minimizes the energy

$$\Phi(\{\mathbf{r}_i\}) = \Phi(\{\mathbf{r}_i^0\}) + \frac{1}{2} \sum_{i,\alpha,j,\beta} \delta r_i^\alpha \mathcal{H}_{i\alpha,j\beta} \delta r_j^\beta + \dots \quad [2]$$

where $\delta r_i^\alpha \equiv r_i^\alpha - r_i^{\alpha,0}$ and we consider only the non-pinned particles. In Eq. (2), we have defined the dynamical matrix

$$\mathcal{H}_{i\alpha,j\beta} \equiv \left. \frac{\partial^2 \phi(r_{ij})}{\partial r_i^\alpha \partial r_j^\beta} \right|_{\{\mathbf{r}_i^0\}}, \quad [3]$$

where the latin indices $i, j = 1, \dots, N$ indicate the particles and greek symbols $\alpha, \beta = 1, \dots, d$ the cartesian coordinates.

The energy minimization has been obtained through the Limited-memory Broyden-Fletcher-Goldfarb-Shanno algorithm (39). For each value of p , we have collected data for 10^2 inherent structures obtained considering different thermalized configuration. At the end of the minimization, we have checked the structural properties of the corresponding configuration through the radial distribution function $g(\mathbf{r}) = \langle N^{-1} \sum_{i \neq j} \delta(\mathbf{r} - \mathbf{r}_j + \mathbf{r}_i) \rangle$.

The normal modes are then obtained thorough the diagonalization of the dynamical matrix \mathcal{H} . For system sizes up to 1024, we evaluate the entire eigenvalue spectrum through *gsl-GNU libraries*, for larger sizes we compute the lowest 100 eigenvalues with ARPACK (40). Indicating with λ_κ the eigenvalues of \mathcal{H} , the corresponding $3N$ squared normal-mode frequencies are $\omega_\kappa^2 = \lambda_\kappa$. From the spectrum of the eigenvalues $\rho(\lambda)$, using the relation between ω_κ and λ_κ , we compute both, the cumulative function $F(\omega)$ and the density of states $D(\omega)$. The cumulative function $F(\omega)$ reads

$$F(\omega) = \int_0^\omega d\omega' D(\omega'). \quad [4]$$

In the case of a three dimensional elastic solid, the spectrum at low frequencies is populated by phonons, that brings to the power law $F(\omega) \sim \omega^d$ and $D(\omega) \sim \omega^{d-1}$. If the low-frequency spectrum is populated by non-Goldstone soft-modes, one expects that $D(\omega)$ reaches zero as a power law with $D(\omega) \sim \omega^\delta$ and, consequently, $F(\omega) \sim \omega^\alpha$, with $\alpha - 1 = \delta$.

As a measure of the spatial extension of the normal modes, we compute the inverse participation ratio $IPR(\omega)$ defined as (41)

$$IPR(\omega) \equiv \frac{\sum_i |\mathbf{e}_i(\omega)|^4}{\left(\sum_i |\mathbf{e}_i(\omega)|^2\right)^2} \quad [5]$$

where $\mathbf{e}_i(\omega)$ is the eigenvector of the mode ω . For a completely localized mode ω on a single particle, one has $IPR(\omega) = 1$, while a mode extended over all the particles corresponds to $IPR(\omega) \sim N^{-1}$.

ACKNOWLEDGMENTS. MP was supported by the Simons Foundation Targeted Grant in the Mathematical Modeling of Living Systems Number: 342354, GP and by the Syracuse Soft & Living Matter Program. This project has received funding from the European Research Council (ERC) under the European Union's Horizon 2020 research and innovation programme (grant agreement No [694925])

1. Kittel C (2005) *Introduction to solid state physics*. (Wiley).
2. Widmer-Cooper A, Perry H, Harrowell P, Reichman DR (2008) Irreversible reorganization in a supercooled liquid originates from localized soft modes. *Nature Physics* 4(9):711–715.
3. Manning ML, Liu AJ (2011) Vibrational modes identify soft spots in a sheared disordered packing. *Physical Review Letters* 107(10):108302.
4. O'Hern CS, Silbert LE, Liu AJ, Nagel SR (2003) Jamming at zero temperature and zero applied stress: The epitome of disorder. *Phys. Rev. E* 68(1):011306.
5. Wyart M (2012) Marginal stability constrains force and pair distributions at random close packing. *Phys. Rev. Lett.* 109(12):125502.
6. Franz S, Parisi G, Urbani P, Zamponi F (2015) Universal spectrum of normal modes in low-temperature glasses. *Proceedings of the National Academy of Sciences* 112(47):14539–14544.
7. Kurchan J, Parisi G, Urbani P, Zamponi F (2013) Exact theory of dense amorphous hard spheres in high dimension. ii. the high density regime and the gardner transition. *The Journal of Physical Chemistry B* 117(42):12979–12994.
8. Charbonneau P, Kurchan J, Parisi G, Urbani P, Zamponi F (2017) Glass and jamming transitions: From exact results to finite-dimensional descriptions. *Annual Review of Condensed Matter Physics* 8:265–288.
9. Mézard M, Parisi G, Sourlas N, Toulouse G, Virasoro M (1984) Nature of the spin-glass phase. *Phys. Rev. Lett.* 52(13):1156–1159.
10. Charbonneau P, Kurchan J, Parisi G, Urbani P, Zamponi F (2014) Fractal free energy landscapes in structural glasses. *arXiv preprint arXiv:1404.6809*.
11. Gurarie V, Chalker JT (2003) Bosonic excitations in random media. *Phys. Rev. B* 68(13):134207.
12. Gurevich VL, Parshin DA, Schober HR (2003) Anharmonicity, vibrational instability, and the boson peak in glasses. *Phys. Rev. B* 67(9):094203.
13. Schirmacher W, Ruocco G, Scopigno T (2007) Acoustic attenuation in glasses and its relation with the Boson Peak. *Physical Review Letters* 98:025501.
14. Shintani H, Tanaka H (2008) Universal link between the boson peak and transverse phonons in glass. *Nature materials* 7(11):870.
15. Lerner E, Gartner L (2016) Nonlinear modes disentangle glassy and goldstone modes in structural glasses. *SciPost Physics* 1(2):016.
16. Baity-Jesi M, Martin-Mayor V, Parisi G, Perez-Gaviró S (2015) Soft modes, localization, and two-level systems in spin glasses. *Phys. Rev. Lett.* 115(26):267205.
17. Lerner E, Düring G, Bouchbinder E (2016) Statistics and properties of low-frequency vibrational modes in structural glasses. *Phys. Rev. Lett.* 117(3):035501.
18. Lerner E, Bouchbinder E (2017) Effect of instantaneous and continuous quenches on the density of vibrational modes in model glasses. *Phys. Rev. E* 96(2):020104.
19. Lerner E, Düring G, Bouchbinder E (2016) Statistics and properties of low-frequency vibrational modes in structural glasses. *Physical review letters* 117(3):035501.
20. Mizuno H, Shiba H, Ikeda A (2017) Continuum limit of the vibrational properties of amorphous solids. *Proceedings of the National Academy of Sciences* 114(46):E9767–E9774.
21. Kob W, Roldán-Vargas S, Berthier L (2012) Non-monotonic temperature evolution of dynamic correlations in glass-forming liquids. *Nature Physics* 8(2):164.
22. Cammarota C, Biroli G (2012) Ideal glass transitions by random pinning. *Proceedings of the National Academy of Sciences* 109(23):8850–8855.
23. Ozawa M, Kob W, Ikeda A, Miyazaki K (2015) Equilibrium phase diagram of a randomly pinned glass-former. *Proceedings of the National Academy of Sciences* 112(22):6914–6919.
24. Kob W, Berthier L (2013) Probing a liquid to glass transition in equilibrium. *Phys. Rev. Lett.* 110(24):245702.
25. Cammarota C, Biroli G (2013) Random pinning glass transition: Hallmarks, mean-field theory and renormalization group analysis. *The Journal of chemical physics* 138(12):12A547.
26. Brito C, Parisi G, Zamponi F (2013) Jamming transition of randomly pinned systems. *Soft Matter* 9(35):8540–8546.
27. Gokhale S, Nagamanasa KH, Ganapathy R, Sood A (2014) Growing dynamical facilitation on approaching the random pinning colloidal glass transition. *Nature communications* 5:4685.
28. Nagamanasa KH, Gokhale S, Sood A, Ganapathy R (2015) Direct measurements of growing amorphous order and non-monotonic dynamic correlations in a colloidal glass-former. *Nature Physics* 11(5):403.
29. Szamel G, Flenner E (2013) Glassy dynamics of partially pinned fluids: An alternative mode-coupling approach. *EPL (Europhysics Letters)* 101(6):66005.
30. DeGiuli E, Lerner E, Brito C, Wyart M (2014) Force distribution affects vibrational properties in hard-sphere glasses. *Proceedings of the National Academy of Sciences* 111(48):17054–17059.
31. Charbonneau P, Corwin EI, Parisi G, Zamponi F (2015) Jamming criticality revealed by removing localized buckling excitations. *Phys. Rev. Lett.* 114(12):125504.
32. Xu N, Vitelli V, Liu AJ, Nagel SR (2010) Anharmonic and quasi-localized vibrations in jammed solids—modes for mechanical failure. *EPL (Europhysics Letters)* 90(5):56001.
33. Schirmacher W, Ruocco G, Mazzone V (2015) Heterogeneous... *Physical Review Letters* 115:015901.
34. Volpe G, Kurz L, Callegari A, Volpe G, Gigan S (2014) Speckle optical tweezers: micromanipulation with random light fields. *Optics express* 22(15):18159–18167.
35. Di Leonardo R, Ianni F, Ruocco G (2007) Computer generation of optimal holograms for optical trap arrays. *Optic Express* 15:1913.
36. Ghosh A, Chikkadi VK, Schall P, Kurchan J, Bonn D (2010) Density of states of colloidal glasses. *Physical review letters* 104(24):248305.
37. Grigera TS, Parisi G (2001) Fast monte carlo algorithm for supercooled soft spheres. *Phys. Rev. E* 63(4):045102.
38. Rosenfeld Y, Tarazona P (1998) Density functional theory and the asymptotic high density expansion of the free energy of classical solids and fluids. *Molecular Physics* 95(2):141–150.
39. Bonnans JF, Gilbert JC, Lemaréchal C, Sagastizábal CA (2006) *Numerical optimization: the theoretical and practical aspects*. (Springer Science & Business Media).
40. Sorensen D, Lehoucq R, Yang C, Maschhoff K (year?) Arnoldi package (arpack). www.caam.rice.edu/software/ARPACK/.

DRAFT